Magnetic reconnection with anomalous resistivity in two-and-a-half dimensions I: Quasi-stationary case

Leonid M. Malyshkin* and Timur Linde†
Department of Astronomy, The University of Chicago – The Center for Magnetic Self-Organization (CMSO), Chicago, IL 60637.

Russell M. Kulsrud‡
Princeton Plasma Physics Laboratory – The Center for Magnetic Self-Organization (CMSO), Princeton, NJ 08543.
(Dated: February 5, 2008)

In this paper quasi-stationary, two-and-a-half-dimensional magnetic reconnection is studied in the framework of incompressible resistive magnetohydrodynamics (MHD). A new theoretical approach for calculation of the reconnection rate is presented. This approach is based on local analytical derivations in a thin reconnection layer, and it is applicable to the case when resistivity is anomalous and is an arbitrary function of the electric current and the spatial coordinates. It is found that a quasi-stationary reconnection rate is fully determined by a particular functional form of the anomalous resistivity and by the local configuration of the magnetic field just outside the reconnection layer. It is also found that in the special case of constant resistivity reconnection is Sweet-Parker and not Petschek.

PACS numbers: 52.30.Cv, 52.35.Vd, 52.65.Kj

I. INTRODUCTION

Magnetic reconnection is the physical process of breaking and rearrangement of magnetic field lines, which changes the topology of the field. It is one of the most fundamental processes of plasma physics and is believed to be at the core of many dynamic phenomena in laboratory experiments and in cosmic space. Unfortunately, in spite of being so important, magnetic reconnection is still relatively poorly understood from the theoretical point of view. The reason is that plasmas usually have very high temperatures and low densities. In such plasmas, the Spitzer resistivity is extremely small and magnetic fields are almost perfectly frozen into cosmic plasmas. As a result, simple theoretical models, such as the Sweet-Parker reconnection model [1, 2] predict that the magnetic reconnection processes should be extremely slow and insignificant throughout the universe. On the other hand, astrophysical observations show magnetic reconnection tends to be fast and is likely to be the primary driver of many highly energetic cosmic processes, such as solar flares and geomagnetic storms. This contradiction between theoretical estimates and astrophysical observations triggered multiple attempts to build a theoretical model of fast magnetic reconnection.

First, in 1964 Petschek proposed a fast reconnection model [3], in which fast reconnection is achieved by introducing switch-off magnetohydrodynamic (MHD) shocks attached to the ends of the reconnection layer in the downstream regions and by choosing the reconnection layer length to be equal to its minimal possible value under the condition of no significant disruption to the plasma flow. However, later numerical simulations and theoretical derivations did not confirm the Petschek theoretical picture for the geometry of a reconnection layer [4–6]. Second, numerical simulations studies of anomalous magnetic reconnection, for which resistivity is enhanced locally in the reconnection layer, were pioneered by Ugai and Tsuda [7, 8], by Hayashi and Sato [9, 10], and by Scholer [11]. Third, Lazarian and Vishniac proposed that fast reconnection can occur in turbulent plasmas [12], although the back-reaction of magnetic fields can slow down reconnection in this case [13]. Finally, recently there have been number of attempts to explain the fast magnetic reconnection by considering non-MHD effects [14–21].

Most previous theoretical and numerical studies concentrated on reconnection processes in two-dimensions or in "two-and-a-half-dimensions". The later is the term used for a problem in which physical scalars and all three components of physical vectors depend only on two spatial coordinates (e.g. x and y) and are independent of the third coordinate (z).

In this paper we consider two-and-a-half-dimensional magnetic reconnection with anomalous resistivity in the classical Sweet-Parker-Petschek reconnection layer, which is shown in the left plot in Fig. 1. The reconnection layer is in the x-y plane with the y-axis being along the layer and the x-axis being perpendicular to the layer. The length of the layer is equal to $2L'$. Note that L' is approximately equal to or smaller than the global magnetic field scale, which we denote as L. The thickness of the classical reconnection layer, $2\delta_o$, is much smaller than its length, i.e. $2\delta_o \ll 2L'$. The classical Sweet-Parker-Petschek reconnection layer is assumed to possess a point symmetry with respect to its geometric

---

*Electronic address: leonmal@flash.uchicago.edu
†Electronic address: linde@flash.uchicago.edu
‡Electronic address: rmk@pppl.gov

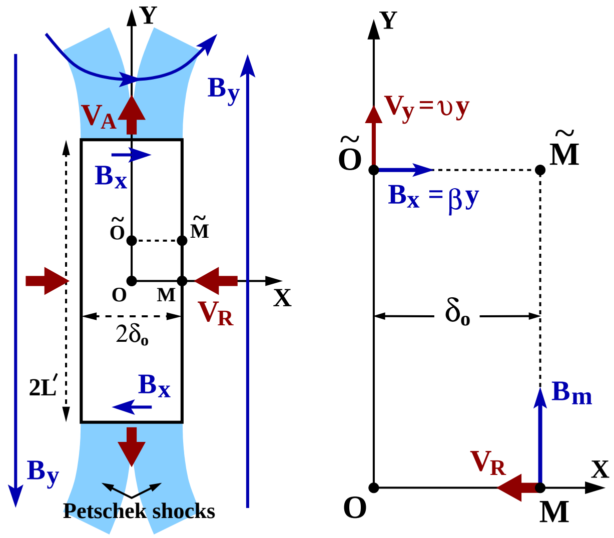

FIG. 1: (Color online) The geometrical configuration of the classical Sweet-Parker-Petschek reconnection layer is shown in the left plot. Petschek shocks exist only if the reconnection is considerably faster than the Sweet-Parker reconnection rate. The right plot shows an enlarged picture of the central layer region.

center point O and reflection symmetries with respect to the axes x and y (refer to Fig. 1). Thus, for example, the x- and y-components of the plasma velocities $\mathbf{V}$ and of the magnetic field $\mathbf{B}$ have the following simple symmetries: $V_x(\pm x, \mp y) = \pm V_x(x, y)$, $V_y(\pm x, \mp y) = \mp V_y(x, y)$, $B_x(\pm x, \mp y) = \mp B_x(x, y)$ and $B_y(\pm x, \mp y) = \pm B_y(x, y)$. There might be a pair of Petschek shocks attached to each of the two reconnection layer ends in the downstream regions (see Fig. 1). Because of the MHD jump conditions on the Petschek shocks, the presence of these shocks requires the presence of a significant perpendicular magnetic field B_x at the reconnection layer ends [5, 22]. The plasma outflow velocity from the reconnection layer is approximately equal to the Alfven velocity V_A (if the plasma viscosity is not very large). The plasma inflow velocity V_R outside of the reconnection layer, at point M in Fig. 1, is much smaller than the outflow velocity, $V_R \ll V_A$. Finally, the magnetic field outside the reconnection layer is mostly in the direction of the layer (i.e. in the y-axis direction).

The problem of quasi-stationary anomalous magnetic reconnection in the classical Sweet-Parker-Petschek reconnection layer was recently theoretically addressed by Kulsrud [5] for the special case of zero guide field ($B_z = 0$), zero plasma viscosity and anomalous resistivity that is a piecewise linear function of the electric current [see Eq. (32)]. There are two major results of the Kulsrud anomalous reconnection model. First, in the case of the Petschek geometry of the reconnection layer and a constant resistivity, one has to calculate the half-length of the reconnection layer L' from the MHD equations and the jump conditions on the Petschek shocks, instead of treating L' as a free parameter (as Petschek did). When the layer half-length L' is calculated correctly, it turns out to be approximately equal to the global magnetic field scale, $L' \approx L$. In this case the Petschek reconnection reduces to the slow Sweet-Parker reconnection [5, 22]. This theoretical result is in agreement with the results of numerical simulations of two-dimensional reconnection with constant resistivity [4, 6]. The second major result of the Kulsrud reconnection model is that in the case when resistivity is anomalous and enhanced (e.g. by plasma instabilities), the reconnection rate becomes considerably faster than the Sweet-Parker rate.

In this paper we develop and use a new theoretical approach for calculation of the reconnection rate in the case of anomalous resistivity. This approach is based on application of the MHD equations in a small region, which is localized at the geometric center of a thin reconnection layer (point O in Fig. 1) and has a size of order of the layer half-thickness δ_o. It turns out that by using local analytical calculations in a thin reconnection layer, we can derive an accurate and rather precise estimate for the reconnection rate. In particular, we find the interesting and important result that a quasi-stationary reconnection rate is fully determined by the anomalous resistivity function and by the magnetic field configuration just outside the reconnection layer (at point M in Fig. 1). The underlying physical foundations of our analytical derivations are, of course, the same as those previously used by others [1, 2, 5]. However, our theoretical and computational approach is somewhat different from the conventional approach to the reconnection problem, and we explain the difference in the next section. There are three main benefits of our novel theoretical approach to magnetic reconnection. First, our approach allows us to extend the results for anomalous reconnection obtained by Kulsrud in 2001 [5] to a general anomalous reconnection case, when the guide field and plasma viscosity are arbitrary and anomalous resistivity η is an arbitrary function of the electric current and the two spatial coordinates. Second, it gives a new important insight into the reconnection problem, such as dependence of the reconnection rate on magnetic field configuration just outside the reconnection layer. Third, our approach, based on local calculations, is applicable to cases when there is no well-defined global magnetic field structure, such as the case of multiple current sheets in a turbulent plasma. In our calculations we make only a few assumptions, which are described in detail in the beginning of Sec. III.

This paper is organized as follows. Because our derivations are rather complicated in the general case of reconnection with anomalous resistivity, we find it useful and instructive to consider the Sweet-Parker reconnection first and to compare our theoretical approach to the classical Sweet-Parker calculations in the next section. In Sec. III, we derive our general equations for magnetic reconnection with anomalous resistivity, including the equation for the reconnection rate. In Sec. IV we consider and analyze different special cases of magnetic reconnec-

tion, in which our equations simplify and become easier for analysis and comparison to the previous theoretical and simulation results. In Sec. V we present the results of our numerical simulations of unforced anomalous magnetic reconnection. These simulations are intended for a demonstration of the predictions of our theoretical reconnection model for the special case of the piecewise linear resistivity function that was considered by Kulsrud [5]. Finally, in Sec. VI we give our conclusions and discuss our results. Some derivations are given in the appendices of the paper.

II. THE SWEET-PARKER MODEL OF MAGNETIC RECONNECTION

For simplicity and brevity, hereafter in the paper for all electromagnetic variables we use physical units in which the speed of light and four times π are replaced unity, $c = 1$ and $4\pi = 1$. To rewrite our equations in the standard CGS units, one needs to make the following substitutions for electromagnetic variables in the equations: magnetic field $\mathbf{B} \to \mathbf{B}/\sqrt{4\pi}$, electric field $\mathbf{E} \to c\mathbf{E}/\sqrt{4\pi}$, electric current $\mathbf{j} \to (\sqrt{4\pi}/c)\mathbf{j}$, resistivity $\eta \to \eta$ (does not change), magnetic field vector potential $\mathbf{A} \to \mathbf{A}/\sqrt{4\pi}$.

In this section we consider Sweet-Parker reconnection [1, 2]. We assume that resistivity is constant, $\eta \equiv \text{const} = \eta_o$, the plasma viscosity is zero, the guide field is zero ($B_z = 0$), and the geometry of the reconnection layer is the classical Sweet-Parker geometry with the layer half-thickness $\delta_o \ll L$ and the layer half-length $L' = L$, as shown in Fig. 1. The purpose of this section is to introduce and explain our new theoretical approach to calculation of the reconnection rate and to compare it with the classical Sweet-Parker calculations. For this purpose, we first present the classical, conventional derivation of the Sweet-Parker formula for the reconnection rate, and afterward we present our new derivation of the formula and explain the difference between the two derivations.

In the case of a quasi-stationary reconnection the magnetic field in the reconnection region changes slowly in time, $\partial\mathbf{B}/\partial t \approx 0$. Therefore, in the two-and-a-half-dimensional geometry ($\partial/\partial z \equiv 0$) the Faraday's law equation $-\nabla \times \mathbf{E} = \partial\mathbf{B}/\partial t \approx 0$ results in the z-component of the electric field being constant in the reconnection region, $\nabla E_z = 0$ and $E_z = E_z(t)$ is a function of time only. On the other hand, in two-and-a-half dimensions the x- and y-components of Faraday's law equation $\partial\mathbf{B}/\partial t = -\nabla \times \mathbf{E} = -\nabla \times (\eta\mathbf{j} - [\mathbf{V} \times \mathbf{B}])$ reduce to the following equation for the z-component of the magnetic vector potential $\mathbf{A}$:

$$\begin{aligned} -E_z(t) &= \partial A_z/\partial t = -(\mathbf{V}\cdot\nabla)A_z + \eta\nabla^2 A_z \\ &= V_x B_y - V_y B_x - \eta j_z. \end{aligned} \tag{1}$$

(The resistivity $\eta \equiv \text{const} = \eta_o$ is constant in the Sweet-Parker reconnection case, but equation (1) is general and is valid even if resistivity η is anomalous and non-constant.)

Now, the left- and right-hand-sides of equation (1) are constant in space. Therefore, the right-hand-side of equation (1) is constant across the reconnection layer (i.e. along the x-axis). We equate its values at points O and M, which are on the x-axis and are shown in Fig. 1. As a result, we immediately obtain

$$\eta_o j_o = V_R B_m, \tag{2}$$

where we use the following notations: Point O is the geometric center of the reconnection layer, where the z-component of the current is $j_o = j_z(x=0, y=0)$ and the plasma velocity is zero. Point M is a point on the x-axis just outside the reconnection layer, where the resistivity term can be neglected in equation (1), see Fig. 1. We also use the notations $B_y = B_m$ and $V_x = -V_R$ for the y-component of the field and x-component of the plasma velocity at point M, and take the reconnection velocity V_R positive. Note that $V_y = B_x = 0$ at point M because of the symmetry of the problem with respect to the x-axis. Next, we estimate current j_o at the central point O of the reconnection layer as

$$j_o \approx B_m/\delta_o, \tag{3}$$

where δ_o is the reconnection layer half-thickness, and we use Ampere's law, $j_o = (\partial B_y/\partial x)_o - (\partial B_x/\partial y)_o \approx (\partial B_y/\partial x)_o \approx B_m/\delta_o$, in which we drop the $(\partial B_x/\partial y)_o$ term because the reconnection layer is thin [36].

Next, consider the x- and y-components of the equation of plasma motion. We will see below that the Sweet-Parker reconnection is slow, $V_R \ll V_A \equiv B_m/\sqrt{\rho}$. Therefore, in the equation of plasma motion along the x-axis (i.e. across the reconnection layer) the inertial term can be neglected, and this equation becomes the force balance equation, $(\partial/\partial x)(P + B^2/2) = 0$, resulting in $P_o = P_m + B_m^2/2$, where P_o and P_m are the values of the plasma pressure at points O and M. Here we use the fact that the magnetic field is zero at the central point O because of the symmetry of the problem. As far as the equation of plasma motion along the y-axis (i.e along the layer) is concerned, the y-components of the magnetic tension force and the pressure gradient force are approximately equal in the Sweet-Parker reconnection case. Indeed, on the y-axis the tension force can be estimated as $(\mathbf{B}\cdot\nabla)B_y = B_x \times (\partial B_y/\partial x) \approx (\delta_o/L)B_m \times (B_m/\delta_o) = B_m^2/L \approx (P_o - P_m)/L \approx -\partial P/\partial y$. Here we estimate the x-component of the field as $B_x \approx (\delta_o/L)B_m$ because B_x is produced by the rotation of the B_y field component in the reconnection layer [5], and in the Sweet-Parker model it is assumed that the downstream pressure is equal to the upstream pressure P_m (see [1, 2]). The pressure and magnetic tension forces accelerate plasma along the reconnection layer (i.e. along the y-axis) up to the downstream velocity V_{out}, which can be estimated from the energy conservation equation

$$(1/2)\rho V_{out}^2 \approx B_m^2/2 \;\;\Rightarrow\;\; V_{out} \approx V_A \equiv B_m/\sqrt{\rho}. \tag{4}$$

This equation means that the work done by the pressure and magnetic tension forces along the entire reconnection layer is equal to the kinetic energy of the plasma in the downstream regions.

Finally, in the Sweet-Parker reconnection model the plasma is assumed to be incompressible. Therefore, the mass conservation condition for the entire reconnection layer results in

$$LV_R \approx \delta_o V_{out}, \tag{5}$$

where V_{out}, the velocity of plasma outflow in the downstream regions, is given by equation (4). Using equations (2)-(5), we obtain the formula for the Sweet-Parker reconnection velocity [1, 2],

$$V_R \approx V_A(\eta_o/V_A L)^{1/2}. \tag{6}$$

Equations (2)-(6) are the classical Sweet-Parker equations. Note that equations (2), (3) and (6) are local, in the sense that they are written for a small region of space, which is localized at the geometric center of a thin reconnection layer (point O in Fig. 1) and has a size of order of the layer half-thickness δ_o. All physical quantities that enter these three equations are defined in this small region of space. At the same time equations (4) and (5) are global, in the sense that they result from consideration of the entire reconnection layer and they include the plasma outflow velocity $V_{\rm out}$, which is a physical quantity in the downstream regions at the ends of the reconnection layer. In our new theoretical approach to the calculation of the reconnection rate we intend to use only local equations. Our intent and our derivations will be justified by the new and important results that we obtain in the next section of this paper and discuss in Sec. VI. At present, let us explain our theoretical approach for the simple case of Sweet-Parker reconnection that we consider in this section.

In the derivation of our theoretical model for magnetic reconnection we keep equations (2) and (3) unchanged because these equations are local. However, we rewrite equations (4) and (5) because they are global. To rewrite these two global equations in a local form, we consider a point $\tilde{\rm O} = (x=0, y=\tilde{y})$ that is located on the y-axis in an infinitesimal vicinity of the reconnection layer central point O (see Fig. 1) and has an infinitesimally small value of its y-coordinate $\tilde{y}$. Since $\tilde{y} \to +0$, along the O$\tilde{\rm O}$ interval we can use the up-to-the-first-order Taylor expansions $B_x(0,y) = \beta y$, $V_y(0,y) = \upsilon y$ and $j_z(0,y) = j_o$ for the values of the perpendicular magnetic field B_x, plasma velocity V_y and z-component of the current j_z. These expansions are along the y-axis, and, of course, $\beta \equiv (\partial B_x/\partial y)_o$ and $\upsilon \equiv (\partial V_y/\partial y)_o$ are the first-order partial derivatives of B_x and V_y at point O (note that $(\partial J_z/\partial y)_o = 0$). Now equation (4) for the plasma acceleration along the y-axis can easily be rewritten in a local form at point $\tilde{\rm O}$ as

$$\begin{aligned} \frac{1}{2}\rho(\upsilon\tilde{y})^2 &\approx \int_0^{\tilde{y}} B_x(0,y) j_z(0,y) dy = \int_0^{\tilde{y}} \beta y j_o dy \\ &= \beta j_o \tilde{y}^2/2 \quad \Rightarrow \quad \rho\upsilon^2 \approx \beta j_o, \end{aligned} \tag{7}$$

where the left-hand-side of this equation is the plasma kinetic energy at point $\tilde{\rm O}$. On the right-hand-side of equation (7) we keep only the magnetic tension force for plasma acceleration because, as we found above, in the Sweet-Parker reconnection case the y-components of the magnetic tension and pressure gradient forces are approximately equal to each other (note that in our general calculations in the next section we will take all forces into account). Next, equation (5) for the mass conservation of an incompressible plasma can easily be rewritten in the local form inside the area OM$\tilde{\rm M}\tilde{\rm O}$ shown in Fig. 1 as $\tilde{y}V_R \approx \delta_o V_y(0,\tilde{y}) = \delta_o \upsilon \tilde{y}$. Thus, we have

$$\upsilon \approx V_R/\delta_o, \quad \text{where } \upsilon \equiv (\partial V_y/\partial y)_o = -(\partial V_x/\partial x)_o. \tag{8}$$

This equation can also be viewed as the first order Taylor expansion of V_x along the x-axis (i.e. across the reconnection layer), $V_R \equiv -V_x(\delta_o, 0) \approx -(\partial V_x/\partial x)_o \delta_o = (\partial V_y/\partial y)_o \delta_o = \upsilon\delta_o$, where we use the plasma incompressibility condition $\partial V_x/\partial x + \partial V_y/\partial y = 0$.

Note that our first and second equations are local and are exactly the same as equations (2) and (3) in the Sweet-Parker reconnection model. Our third and fourth equations (7) and (8) are also local and are the analogues of the two global Sweet-Parker equations (4) and (5). Using local equations instead of global ones is the first major difference between the Sweet-Parker and our theoretical models. However, in our theoretical model we have an additional unknown parameter $\beta \equiv (\partial B_x/\partial y)_o$, which does not directly enter the classical Sweet-Parker reconnection model. As a result, we need one additional equation to be able to calculate the reconnection rate under the framework of our local model. This additional equation comes from the condition that the right-hand-side of equation (1) is constant not only across the reconnection layer, but also along the layer that is along the y-axis. This condition is not explicitly used in the Sweet-Parker model, but it is used in our model, and this is the second major difference between the two models. To derive the additional equation, used in our reconnection model, we differentiate the left- and right-hand-sides of equation (1) along the y-axis (i.e. along the reconnection layer). The first order partial derivatives $\partial/\partial y$ are identically zero because of the symmetry of the problem with respect to the x-axis. The second order partial derivatives $\partial^2/\partial y^2$ of the left- and right-hand-sides of equation (1) result in

$$\begin{aligned} 0 &= -2(\partial V_y/\partial y)_o(\partial B_x/\partial y)_o - \eta_o(\partial^2 j_z/\partial y^2)_o \\ &\approx -2\upsilon\beta + 2\eta_o j_o/L^2, \end{aligned} \tag{9}$$

where we use the fact that $V_x = B_y = 0$ on the y-axis, we use our definitions $\beta \equiv (\partial B_x/\partial y)_o$ and $\upsilon \equiv (\partial V_y/\partial y)_o$, and we estimate the second derivative of the current j_z as $(\partial^2 j_z/\partial y^2)_o \approx -2j_o/L^2$. Now all five equations (2), (3), (7)-(9) are local. Combining them together, we easily obtain the Sweet-Parker formula for the reconnection velocity, given by equation (6), which is naturally also local, see Ref. [37].

The reader of this paper could question why we develop and suggest a new theoretical approach to the problem of quasi-stationary magnetic reconnection if we obtain the same results in the Sweet-Parker reconnection case. The answer is that our approach, based on local calculations, allows us to calculate the reconnection rate in the case of anomalous resistivity and also provides an additional important understanding of the reconnection problem. Our derivations for anomalous reconnection are given in the next section and we discuss our results in Sec. VI. Note that our local-equations approach to the reconnection problem and the more conventional global-equations approach are the same from the point of view of the underlying physics. Indeed, it is well known that by using the Gauss-Ostrogradski theorem, most physical equations can be written in two equivalent forms, in the form of local differential equations and in the form of global integral equations.

III. MAGNETIC RECONNECTION WITH ANOMALOUS RESISTIVITY

In this section we study reconnection with anomalous resistivity and derive a simple and accurate estimate of the reconnection rate in the classical Sweet-Parker-Petschek two-and-a-half dimensional reconnection layer shown in Fig. 1. We consider resistivity to be a given arbitrary function of the z-component of the electric current and the two-dimensional coordinates, $\eta = \eta(j_z, x, y)$, which has finite derivatives in y up to the second order and in x and j_z up to the first order [38].

Let us list the assumptions that we make. First, we assume that the characteristic Lundquist number of the problem is large, which (by our definition) is equivalent to the assumption that resistivity is negligible outside the reconnection layer and the non-resistive MHD equations apply there. Second, we assume that the plasma flow is incompressible, $\operatorname{div}\mathbf{V} = 0$. In the limit of very high Lundquist numbers and slow reconnection rates the incompressibility condition is a very good approximation in a reconnection layer even for compressible plasmas [23]. Third, we assume that the reconnection process is quasi-stationary. This can only be the case if the reconnection rate is small, $\eta_o j_o/V_A B_m \approx V_R/V_A \ll 1$ [$V_A \equiv B_m/\sqrt{\rho}$ and see Eq. (2)], and there are no plasma instabilities in the reconnection layer. Note that in our model the reconnection rate can still be much faster than the Sweet-Parker rate. Fourth, we assume that the reconnection layer is thin, $\delta_o/L' \ll 1$. If plasma kinematic viscosity is small (in comparison with resistivity), then the plasma outflow velocity in the downstream regions is equal to the Alfven velocity V_A, we have plasma mass conservation condition $\delta_o/L' \approx V_R/V_A$, and this assumption of a thin reconnection layer is fully equivalent to the previous assumption of a small reconnection rate. However, if plasma is very viscous, then the plasma outflow velocity is smaller than V_A and assumption $\delta_o/L' \ll 1$ is stronger than assumption $V_R/V_A \ll 1$. Finally, note that we make no assumptions about the values of the guide field B_z and the plasma viscosity. [However, below we will see that our assumption of a quasi-stationary reconnection process in a thin current sheet layer results in a necessary condition $\nu \ll \eta_o(V_A/V_R)$ for the plasma kinematic viscosity ν. Refer to Eq. (27) for more details.]

Now note that several equations that we derived in the previous section for the case of the Sweet-Parker reconnection with constant resistivity stay the same in the case of anomalous resistivity. Indeed, equation (1) stays valid when the resistivity η is not constant. Therefore, equation (2) also stays valid, except that η_o now is the value of resistivity at the reconnection layer central point O (see Fig. 1), i.e. $\eta_o = \eta(j_z = j_o, x = 0, y = 0)$. Equations (3) and (8), which result from the Ampere's law and the plasma incompressibility respectively, obviously stay valid too [39]. At the same time, in the general case of anomalous resistivity that we consider in this section, we need to re-derive equations (7) and (9), which are the equations of the plasma acceleration and spatial homogeneity of the electric field z-component along the reconnection layer (i.e. along the y-axis). However, before we re-derive these two equations, we would first like to derive the equation of magnetic energy conservation. Using Eqs. (2), (3) and (8), we immediately obtain

$$
\upsilon B_m^2 = \epsilon\, \eta_o j_o^2, \quad \epsilon \approx 1, \tag{10}
$$

where for the purpose of comparison of our theoretical results to our numerical simulations we introduce a coefficient ϵ, which is of order of unity. Equation (10) is the equation for magnetic energy conservation. The rate of the supply of magnetic energy into the reconnection layer is equal to the rate of its Ohmic dissipation inside the layer.

Next we derive the equation of plasma acceleration along the reconnection layer (i.e. along the y-axis), taking into consideration all forces acting on the plasma. The MHD equation for the y-component of the plasma velocity V_y, assuming the quasi-stationarity of the reconnection ($\partial/\partial t = 0$) and plasma incompressibility ($\operatorname{div}\mathbf{V} = 0$), is [24]

$$
\begin{aligned}
\rho(\mathbf{V}\cdot\nabla)V_y &= -(\partial/\partial y)\left(P + B_x^2/2 + B_y^2/2\right) \\
&\quad + (\mathbf{B}\cdot\nabla)B_y + \rho\nu\nabla^2 V_y,
\end{aligned} \tag{11}
$$

where ρ is the plasma density, ν is the plasma kinematic viscosity (assumed to be constant) and P is the sum of the plasma pressure and the guide field pressure $B_z^2/2$. Taking the first order partial derivative $\partial/\partial y$ of equation (11) at the central point O, we obtain

$$
\rho\upsilon^2 = -(\partial^2 P/\partial y^2)_o + \beta j_o + \rho\nu\left[\nabla^2(\partial V_y/\partial y)\right]_o, \tag{12}
$$

where we use parameter $\beta \equiv (\partial B_x/\partial y)_o$ and the Ampere's law $j_o = (\partial B_y/\partial x)_o - (\partial B_x/\partial y)_o$ at point O, and we also use the formulas $V_x \equiv B_y \equiv 0$ on the y-axis, and $V_y = B_x = 0$ at point O, which follow from the symmetry of the problem with respect to the x- and y-axes.

The pressure term $(\partial^2 P/\partial y^2)_o$ on the right-hand-side of equation (12) can be precisely calculated in analogy with the Sweet-Parker derivation of the pressure decline along the reconnection layer, which employs the force balance condition for the plasma across the reconnection layer and leads to equation (4). The viscosity term $\rho\nu\left[\nabla^2(\partial V_y/\partial y)\right]_o$ in equation (12) can be calculated approximately by using estimates for the V_y velocity derivatives. In Appendix A we carry out these calculations and show that the pressure and viscosity terms are equal to

$$\begin{aligned}(\partial^2 P/\partial y^2)_o &= B_m(\partial^2 B_y/\partial y^2)_m \\ &\quad + \mathrm{o}\{\rho\upsilon^2, \beta j_o, \rho\nu\upsilon/\delta_o^2\}, \qquad (13)\\ \rho\nu\left[\nabla^2(\partial V_y/\partial y)\right]_o &\approx -\rho\nu\upsilon/\delta_o^2, \qquad (14)\end{aligned}$$

where $B_m(\partial^2 B_y/\partial y^2)_m$ is calculated just outside the reconnection layer at point M (see Fig. 1), and expression $\mathrm{o}\{\rho\upsilon^2, \beta j_o, \rho\nu\upsilon/\delta_o^2\}$ denotes terms that are small compared to either $\rho\upsilon^2$ or βj_o or $\rho\nu\upsilon/\delta_o^2$ in the limit of a slow reconnection rate in a thin reconnection layer, see Ref. [40]. Substituting equations (13) and (14) into equation (12) and using equation (3) for δ_o, we obtain

$$\rho\upsilon^2 \approx -B_m(\partial^2 B_y/\partial y^2)_m + \beta j_o - \rho\nu\upsilon j_o^2/B_m^2, \qquad (15)$$
$$\text{where } \beta \equiv (\partial B_x/\partial y)_o \text{ at point O.}$$

Note that this equation is exact if plasma viscosity can be neglected ($\nu = 0$).

Now we use the condition of spatial homogeneity of the electric field z-component along the reconnection layer, i.e. along the y-axis. We take the second order partial derivatives $\partial^2/\partial y^2$ of the left- and right-hand-sides of equation (1) at the central point O (note that the first order partial derivatives are identically zero). Taking into account the symmetry of the problem, so that $V_x \equiv B_y \equiv 0$ on the y-axis, and $V_y = B_x = \partial j_z/\partial y = 0$ at point O, we obtain

$$\begin{aligned}&-\left[\eta_o + j_o(\partial\eta/\partial j_z)_o\right](\partial^2 j_z/\partial y^2)_o - j_o(\partial^2\eta/\partial y^2)_o \\ &\qquad = 2(\partial V_y/\partial y)_o(\partial B_x/\partial y)_o = 2\upsilon\beta, \qquad (16)\end{aligned}$$

where we use formulas $\upsilon \equiv (\partial V_y/\partial y)_o$ and $\beta \equiv (\partial B_x/\partial y)_o$. Finally, we need to estimate the $(\partial^2 j_z/\partial y^2)_o$ term, which enters the left-hand-side of equation (16). This estimation can be done by taking the second order partial derivative $\partial^2/\partial y^2$ of equation (3), while keeping δ_o constant because the partial derivative in y is to be taken at a constant value $x = \mathrm{const} = \delta_o$. In Appendix B we give the detailed derivations and find that the y-scale of the current j_z is about the same as the y-scale of the outside magnetic field, i.e. $j_o^{-1}(\partial^2 j_z/\partial y^2)_o \approx B_m^{-1}(\partial^2 B_y/\partial y^2)_m$. However, for the purpose of comparison of our theoretical results to numerical simulations in Sec. V, we find it convenient to write

$$j_o^{-1}(\partial^2 j_z/\partial y^2)_o = \gamma B_m^{-1}(\partial^2 B_y/\partial y^2)_m, \quad \gamma \approx 1, \qquad (17)$$

where we introduce the coefficient γ, which is of order unity.

Let us take the dimensionless coefficients ϵ and γ, which enter equations (10) and (17), and are of order unity, to be exactly unity, $\epsilon = 1$ and $\gamma = 1$. Now we have all the equations necessary to determine all unknown physical parameters. In particular, using Eqs. (10), (15), (16) and (17), we easily obtain the following approximate algebraic equation for the z-current j_o at the reconnection layer central point O:

$$\begin{aligned}&3 + \frac{j_o(\partial\eta/\partial j_z)_o}{\eta_o} + \frac{B_m(\partial^2\eta/\partial y^2)_o}{\eta_o(\partial^2 B_y/\partial y^2)_m} \\ &\qquad \approx -\left(1 + \frac{\nu}{\eta_o}\right)\frac{\eta_o^2 j_o^4}{V_A^2 B_m^4}\frac{2B_m}{(\partial^2 B_y/\partial y^2)_m}, \qquad (18)\end{aligned}$$

where the Alfven velocity V_A is defined as $V_A \equiv B_m/\sqrt{\rho}$ and $\eta_o = \eta(j_z = j_o, x = 0, y = 0)$ is the resistivity at point O. Given the resistivity function $\eta = \eta(j_z, x, y)$, as well as the magnetic field B_m and its second order derivative $(\partial^2 B_y/\partial y^2)_m$ outside the reconnection layer, we can solve equation (18) for the current j_o and find the reconnection rate, which is the rate of destruction of magnetic flux at point O, equal to $-(\partial A_z/\partial t)_o$. Using Eq. (1), we find that the reconnection rate is equal to $\eta_o j_o = E_z$. Note that for the classical reconnection layer that we consider (see Fig. 1) the right-hand-side of equation (18) is positive because $2B_m/(\partial^2 B_y/\partial y^2)_m \approx -L^2 < 0$, where L is the global scale of the magnetic field outside the reconnection layer. Once the current j_o is calculated by means of equation (18), we can easily calculate all other reconnection parameters, using Eqs. (2), (3), (8) and (15),

$$\begin{aligned}V_R &\approx \eta_o j_o/B_m \ll V_A, \qquad (19)\\ \upsilon &\approx \eta_o j_o^2/B_m^2, \qquad (20)\\ \beta &\approx j_o\left[(1 + \nu/\eta_o)(\eta_o j_o/V_A B_m)^2\right. \\ &\qquad \left. + (B_m/j_o^2)(\partial^2 B_y/\partial y^2)_m\right] \ll j_o, \qquad (21)\\ \delta_o &\approx B_m/j_o \approx V_R/\upsilon. \qquad (22)\end{aligned}$$

Equations (18)-(22) are the most general result for magnetic reconnection that we obtain in this paper. Restoring coefficients $\epsilon \approx 1$ and $\gamma \approx 1$, equation (18) becomes

$$\begin{aligned}&(\gamma + 2\epsilon) + \gamma\frac{j_o(\partial\eta/\partial j_z)_o}{\eta_o} + \frac{B_m(\partial^2\eta/\partial y^2)_o}{\eta_o(\partial^2 B_y/\partial y^2)_m} \\ &\qquad = -\epsilon^2\left(\epsilon + \frac{\nu}{\eta_o}\right)\frac{\eta_o^2 j_o^4}{V_A^2 B_m^4}\frac{2B_m}{(\partial^2 B_y/\partial y^2)_m}. \qquad (23)\end{aligned}$$

Hereafter we will consider the natural case when $(\partial\eta/\partial j_z)_o \geq 0$ and $(\partial^2\eta/\partial y^2)_o \leq 0$ because plasma conductivity decreases as the current increases and we are interested in fast anomalous reconnection (i.e. faster than the Sweet-Parker reconnection). In this case the first, second and third terms on the left-hand-side of equation (18) are all positive. It is easy to see that the first term is related to Sweet-Parker reconnection with constant resistivity equal to η_o, the second term is related to fast reconnection associated with the dependence of

anomalous resistivity on the current, and the third term is related to fast reconnection associated with an *ad hoc* localization of resistivity in space (see the next section for details). Also note that if the plasma kinematic viscosity ν is larger than the resistivity η_o, then, according to equation (18), the current j_o and reconnection rate $\eta_o j_o$ become smaller as ν grows, i.e. the reconnection slows down for viscous plasmas as one expects.

We postpone the analysis of equations (18)-(22) until Sec. VI. Let us now make an estimate of the half-length of the reconnection layer L' (see Fig. 1). Note that L' is not needed for the calculation of the reconnection rate $\eta_o j_o$ by means of equation (18). Nevertheless, we are still interested in a rough estimate of L', in particular, because we need to check our assumption that the reconnection layer is thin, i.e. that the condition $\delta_o \ll L'$ is satisfied. It is clear that L' can not be much larger than the global scale of the magnetic field outside the layer L. Therefore we have the condition $L' \lesssim L$. However, L' can be much smaller than L, in which case the reconnection layer has a pair of the Petschek switch-off MHD shocks attached to each end of the layer in the downstream regions [3, 5, 25], as shown in Fig. 1. In this case L' should be calculated as the y-coordinate of the point on the y-axis at which the perpendicular field B_x is strong enough to support the shocks [5]. Following Kulsrud [5], we use the jump condition on the Petschek switch-off shocks to obtain [41]

$$V_R \approx B_x(0, y = L')/\sqrt{\rho} \approx \beta L'/\sqrt{\rho} = \beta L' V_A/B_m, \quad (24)$$

where we use the first-order Taylor expansion for an estimate $B_x(0, y = L') \approx (\partial B_x/\partial y)_o L' = \beta L'$ and, as before, $V_A \equiv B_m/\sqrt{\rho}$. Now, using Eqs. (19), (21) and (24), we can easily find L'. Before we write the explicit formula for L', note that the absolute value of the $(B_m/j_o^2)(\partial^2 B_y/\partial y^2)_m$ term in equation (21) is equal or smaller than the $(1 + 2\nu/\eta_o)(\eta_o j_o/V_A B_m)^2$ term. This follows from the fact that the left-hand-side of equation (18) is equal or greater than unity [see our comments in the paragraph that follows Eq. (23)]. Therefore, the $(B_m/j_o^2)(\partial^2 B_y/\partial y^2)_m$ term can be omitted in equation (21) for the purpose of estimating L'. As a result, we obtain the following rough estimates for the reconnection layer half-length L' and the velocity of plasma outflow in the downstream regions V_{out}:

$$\begin{aligned} L' &\approx (V_A B_m^2/\eta_o j_o^2)(1 + \nu/\eta_o)^{-1} \\ &\approx (V_A/\upsilon)(1 + \nu/\eta_o)^{-1}, \qquad \delta_o \ll L' \lesssim L, \quad (25) \\ V_{out} &\approx \upsilon L' \approx V_A(1 + \nu/\eta_o)^{-1} \le V_A, \quad (26) \end{aligned}$$

where we use equations (19), (20), (21) and (24). Note that the condition $L' \lesssim L$ is always satisfied because $2B_m/(\partial^2 B_y/\partial y^2)_m \approx -L^2$, and the left- and right-hand-sides of equation (18) are equal or greater than unity. However, the condition that the reconnection layer is thin, $\delta_o \ll L'$, is satisfied only if plasma viscosity is not too large,

$$\nu \ll \eta_o(V_A B_m/\eta_o j_o) \approx \eta_o(V_A/V_R), \quad (27)$$

where, to derive this formula, we use Eqs. (19), (22) and (25). In other words, to be able to form a thin reconnection layer, the plasma should not be too viscous. Note that in the case of constant resistivity and large viscosity, η_o = const and $\nu \gg \eta_o$, the reconnection velocity is $V_R/V_A \approx (\eta_o/V_A L)^{1/2}(\eta_o/\nu)^{1/4}$ (see [26]) and condition (27) reduces to $\nu \ll \eta_o(V_A L/\eta_o)^{2/3} = V_A L(\eta_o/V_A L)^{1/3}$. Finally, if the plasma viscosity is small in comparison to the resistivity, $\nu \ll \eta_o$, then from equation (26) we immediately find an important and well-known result that in this case the velocity of the plasma outflowing in the downstream regions at the ends of the reconnection layer is approximately equal to the Alfven velocity, $V_{out} \approx V_A$ (see Fig. 1).

At the end of this section we would like to discuss several assumptions that we used in our derivations. First, the solution of equation (18) is valid only if it gives $\eta_o j_o \ll V_A B_m$, which is our assumption of a slow quasi-stationary reconnection. Because of equation (19), condition $\eta_o j_o \ll V_A B_m$ is equivalent to $V_R \ll V_A$, i.e. the reconnection velocity, which is the velocity of the incoming plasma, must be small in comparison to the Alfven velocity in the upstream region. Second, the coefficient $\beta \equiv (\partial B_x/\partial y)_o$, given by Eq. (21), must be much smaller than the current $j_o = (\partial B_y/\partial x)_o - \beta \approx (\partial B_y/\partial x)_o$ because the reconnection layer is assumed to be thin. It is easy to see that this condition is satisfied. Indeed, the first term in the brackets [...] in equation (21) is much smaller than unity because of the upper limit for plasma viscosity given by equation (27). The second term in the brackets in equation (21) is also much smaller than unity because j_o is much larger than the electric current outside the reconnection layer due to our assumption of a large characteristic Lundquist number of the system.

IV. SPECIAL CASES OF MAGNETIC RECONNECTION

In this section we focus on three special cases for the reconnection rate, which arise when one of the three terms on the left-hand-side of equation (18) dominates over the other two. We consider the classical Sweet-Parker-Petschek reconnection layer shown in Fig. 1 and define the global scale of the magnetic field outside the reconnection layer as $L \equiv \sqrt{-2B_m/(\partial^2 B_y/\partial y^2)_m}$ (see [42]). In addition, for the purpose of clarity, in this section we focus only on resistivity effects and neglect plasma viscosity, assuming that $\nu \ll \eta_o$.

A. Sweet-Parker reconnection, η = const

First, consider the case when resistivity is constant, $\eta(j_z, x, y) = \eta_o$ = const. In this case only the first term on the left-hand-side of equation (18) is nonzero

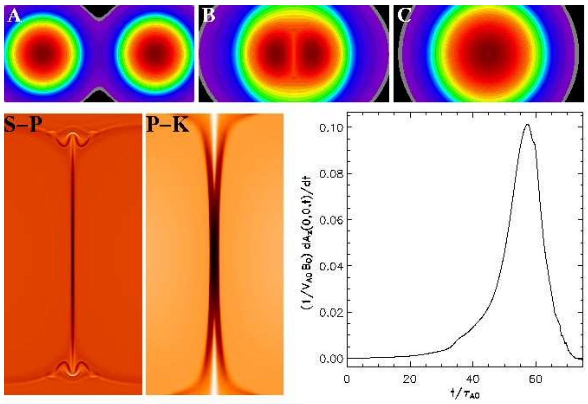

FIG. 2: (Color online) Three top plots: merging of two cylindrical magnetic flux tubes by reconnection (A_z is plotted). Two bottom-left plots: the configuration of the reconnection layer for the Sweet-Parker ("S-P") and Petschek-Kulsrud ("P-K") cases (j_z is plotted). The bottom-right plot: the reconnection rate $dA_z/dt = \eta_o j_o$ at the layer central point O, normalized by $V_{A0}B_0$.

and equations (18)-(22) and (25) reduce to

$$
\begin{array}{ll}
3^{1/2} \approx \eta_o j_o^2 L/V_A B_m^2 \quad \Rightarrow & j_o \approx (B_m/L) S_o^{1/2}, \\
S_o \equiv V_A L/\eta_o \gg 1, & V_R \approx V_A S_o^{-1/2}, \\
\upsilon \approx V_A/L, & \beta \approx (B_m/L) S_o^{-1/2}, \\
\delta_o \approx L S_o^{-1/2}, & L' \approx L,
\end{array}
\qquad (28)
$$

where we set the plasma kinematic viscosity to zero ($\nu = 0$), use our definition of the global field scale $L \equiv \sqrt{-2B_m/(\partial^2 B_y/\partial y^2)_m}$, introduce the Lundquist number $S_o \equiv V_A L/\eta_o$ and assume for our estimates that $3^{1/4} \approx 1$. The above equations are the Sweet-Parker reconnection equations with constant resistivity equal to η_o. Thus, we find that if resistivity is constant, then the reconnection must be Sweet-Parker and not Petschek [5, 22]. We discuss this important result in Sec. VI. Note that in this section, contrary to Sec. II, we do not assume the Sweet-Parker geometrical configuration for the reconnection layer, but derive it together with the reconnection rate from our general equations of the previous section. A typical configuration of the reconnection layer in the case of Sweet-Parker reconnection is shown on the left-bottom plot in Fig. 2. This plot is marked by letters "S-P".

B. Petschek-Kulsrud reconnection, $\eta = \eta(j_z)$

Now let us consider the case when resistivity is anomalous and is a monotonically increasing function of the electric current only, $\eta = \eta(j_z)$. Let us further assume that this dependence of resistivity on the current is very strong, so that $(j_o/\eta_o)(d\eta/dj_z)_o \gg 1$. In this case the second term on the left-hand-side of equation (18) is dominant, and equations (18) and (25) reduce to

$$
\begin{aligned}
(d\eta/dj_z)_o &\approx \eta_o^3 j_o^3 L^2/V_A^2 B_m^4 \quad \Rightarrow \\
\frac{V_R}{V_A} &\approx \frac{\eta_o j_o}{V_A B_m} \approx \frac{\delta_o}{L'} \approx \left[\frac{B_m}{V_A L^2}\left(\frac{d\eta}{dj_z}\right)_o\right]^{1/3}, \qquad (29) \\
L' &\approx \frac{V_A B_m^2}{\eta_o j_o^2} \equiv L\frac{(\eta_o j_o/V_A B_m)^{-3/2}}{(V_A j_o L^2/\eta_o B_m)^{1/2}} \\
&\approx L\left[\frac{j_o}{\eta_o}\left(\frac{d\eta}{dj_z}\right)_o\right]^{-1/2} \ll L. \qquad (30)
\end{aligned}
$$

Here again we set $\nu = 0$, and we use the formula $L^2 \equiv -2B_m/(\partial^2 B_y/\partial y^2)_m$ and Eqs. (19) and (22). From equation (30) we see that the half-length of the reconnection layer L' is much less than the global field scale L in the case of a strong dependence of resistivity on the current ($(j_o/\eta_o)(d\eta/dj_z)_o \gg 1$). This means that in this case the geometry of the reconnection layer is Petschek with a pair of shocks attached to each end of the layer in the downstream regions, as shown in Fig. 1. Equation (29) for the reconnection rate was first analytically derived by Kulsrud [5] for a special case when $d\eta/dj_z \equiv \text{const} = \eta_\star/j_c$. In the Petschek-Kulsrud reconnection case the reconnection rate, given by Eq. (29), can be considerably faster than the Sweet-Parker reconnection rate. This fast reconnection has been previously observed in many numerical simulations done with anomalous resistivity $\eta = \eta(j_z)$ (e.g. see [9, 10, 27]). The typical configuration of the reconnection layer in the case of Petschek-Kulsrud reconnection is shown in the left-bottom plot in Fig. 2, this plot is marked by letters "P-K".

C. Spatially localized reconnection, $\eta = \eta(x, y)$

Finally let us consider the special case when resistivity is given by $\eta = \eta(x, y)$ and it is spatially localized around the central point O of the reconnection layer (see Fig. 1), so that $-2\eta_o/(\partial^2\eta/\partial y^2)_o \equiv l_\eta^2 \ll L^2 \equiv -2B_m/(\partial^2 B_y/\partial y^2)_m$. In other words, we assume that resistivity is anomalous and is localized on scale l_η that is much smaller than the global field scale L. In this case the third term on the left-hand-side of equation (18) is dominant, and equations (18)-(22) and (25) reduce to

$$
\begin{array}{ll}
L/l_\eta \approx \eta_o j_o^2 L/V_A B_m^2 \quad \Rightarrow & j_o \approx (B_m/l_\eta) S_l^{1/2}, \\
S_l \equiv V_A l_\eta/\eta_o \gg 1, & V_R \approx V_A S_l^{-1/2}, \\
\upsilon \approx V_A/l_\eta, & \beta \approx (B_m/l_\eta) S_l^{-1/2}, \\
\delta_o \approx l_\eta S_l^{-1/2}, & L' \approx l_\eta \ll L,
\end{array}
\qquad (31)
$$

where we again set $\nu = 0$. The above equations are the same as the Sweet-Parker equations (28) with the global field scale L replaced by the resistivity scale $l_\eta \ll L$. Note that, when resistivity is localized, the reconnection rate becomes faster than the Sweet-Parker rate by a factor $\sqrt{L/l_\eta} \gg 1$ and the geometry of the reconnection layer

is Petschek with a pair of shocks attached to each end of the layer (see Fig. 1). These results are in agreement with many previous numerical simulations of reconnection with spatially localized resistivity [7, 8, 11, 28].

V. NUMERICAL SIMULATIONS OF MAGNETIC RECONNECTION

In this section we present the results of our numerical simulations of unforced reconnection of two cylindrical magnetic flux tubes. These simulations are not intended as a check or a proof of our theoretical results for magnetic reconnection. Our equations (18)-(22) have been derived analytically and are very general. A comprehensive testing of them would require extensive computational work, which is beyond the scope of this paper. Instead, we present our simulations as a demonstration of our reconnection model predictions.

Following Kulsrud [5], we assume that plasma resistivity is given by the following piecewise linear function of the z-component of the electric current:

$$\eta(j_z) = \eta_s + \eta_\star \max\{0, j_z - j_c\}/j_c, \tag{32}$$

where η_s is the Spitzer resistivity, which is assumed to be very small, $\eta_\star$ is the anomalous resistivity parameter and j_c is the critical current parameter. The Kulsrud model's prediction for the reconnection rate in the case $(j_o/\eta_o)(d\eta/dj_z)_o = j_o\eta_\star/\eta_o j_c \gg 1$, which is given by equation (29), has already been checked and confirmed numerically by Breslau and Jardin [27]. Here we simulate reconnection with anomalous resistivity given by equation (32) for a different computational setup, a higher Lundquist number and a wider range of parameters $\eta_\star$ and j_c (without the restriction $j_o\eta_\star/\eta_o j_c \gg 1$). Our intent is to see how our general formula (18) for the reconnection rate works in this case.

We consider an unforced reconnection of two cylindrical magnetic flux tubes with the initial z-component of the magnetic field vector potential equal to

$$\begin{aligned} A_z(x,y) &= A_0\left[\exp\left(-r_+^2/2R_0^2\right) + \exp\left(-r_-^2/2R_0^2\right)\right], \\ A_0 &= B_0 R_0\sqrt{e}, \quad r_\pm^2 = (x \mp d)^2 + y^2, \end{aligned} \tag{33}$$

see the top-left plot in Fig. 2. This convenient computational setup was suggested to us by Mikic and Vainshtein [29]. We choose the parameters in equation (33) as $R_0 = 1$ (the global scale of the field is unity), $d = 2.7162$ (5% of initially reconnected flux) and $B_0 = 1$ (the maximal initial field is unity). Thus, $A_0 = \sqrt{e}$. In addition, for convenience we choose the plasma density $\rho_0 = 1$, so that the typical Alfven velocity and time are unity, $V_{A0} \equiv B_0/\sqrt{\rho_0} = 1$ and $\tau_{A0} \equiv R_0/V_{A0} = 1$. The guide field is chosen to be zero, $B_z = 0$, and the initial plasma velocities are zero. The initial gas pressure P is chosen in such way that each of the two cylindrical magnetic flux tubes (33) would initially be in complete equilibrium, $P + B_x^2/2 + B_y^2/2 = \text{const}$, if there were no magnetic forces from the other tube. The plasma kinematic viscosity is chosen to be equal to the Spitzer resistivity, $\nu = \eta_s$. The boundary conditions are placed at $x, y = \pm 25$, which are virtually at infinity (the magnetic vector potential (33) drops to less than 10^{-100} at the boundaries). Because of the symmetry of the problem, in the case of a quasi-stationary reconnection considered here, it is enough to run simulations only in the upper-right quadrangle of the full computational box. We use the FLASH code for our simulations. This is a compressible adaptive-mesh-refinement (AMR) code written and supported at the ASC Center of the University of Chicago. (For a comprehensive description of the FLASH code see [30, 31]). The MHD module of the code uses central finite differences to properly resolve all resistive and viscous scales. Comparing numerical results obtained by simulations done with a compressible code to our approximate theoretical formulas derived for incompressible fluids is fine in a case of a very high Lundquist number. This is because in this case the incompressibility condition is a very good approximation in a reconnection layer even for compressible plasmas [23]. Indeed, in our simulations the plasma density varies by no more than 15% inside the reconnection layer. The biggest advantage of the FLASH code for our purposes is that it is an already existing, well tested code with the AMR feature, which allows us to place the boundary conditions at infinity. The size of the smallest elementary grid cell in our two-dimensional simulations was chosen typically to vary from $25/2^{15} = 0.0007629$ to $25/2^{13} = 0.003052$, which was sufficient to resolve the resistive reconnection layer.

The two cylindrical magnetic flux tubes, initially set up according to equation (33), attract each other (in a similar way as two wires with colliniar currents do). As a result, as time goes on, the tubes move toward each other, form a thin reconnection layer along the y-axis and eventually completely merge together by reconnection. This merging process is displayed in the three top plots in Fig. 2, which show the field vector potential A_z in a central region of the full computational box. The two bottom-left plots in Fig. 2 show the electric current j_z in a central region that includes the reconnection layer. These plots clearly show the reconnection layer configuration which is formed during the reconnection process in the cases of the Sweet-Parker and Petschek-Kulsrud reconnection (refer to Secs. IV A and IV B). The bottom-right plot in Fig. 2 demonstrates the functional dependence on time typical of the normalized reconnection rate $(1/V_{A0}B_0)dA_z/dt = \eta_o j_o/V_{A0}B_0$ at the reconnection layer central point O. (This point is shown in Fig. 1). Next we compare the maximal (peak) reconnection rate observed in the numerical simulations with the theoretical rate predicted by our reconnection model.

When resistivity is given by equation (32) and $\nu = \eta_s$, our theoretical formula (18) for the reconnection rate reduces to

$$3 + \frac{\eta_\star}{j_c}\frac{j_o}{\eta_o} \approx (1 + \eta_s/\eta_o)\frac{\eta_o^2 j_o^4 R_0^2}{V_{A0}^2 B_0^4}\,\frac{B_0^6}{B_m^6}\,\frac{L^2}{R_0^2}\,\frac{\rho}{\rho_0}, \tag{34}$$

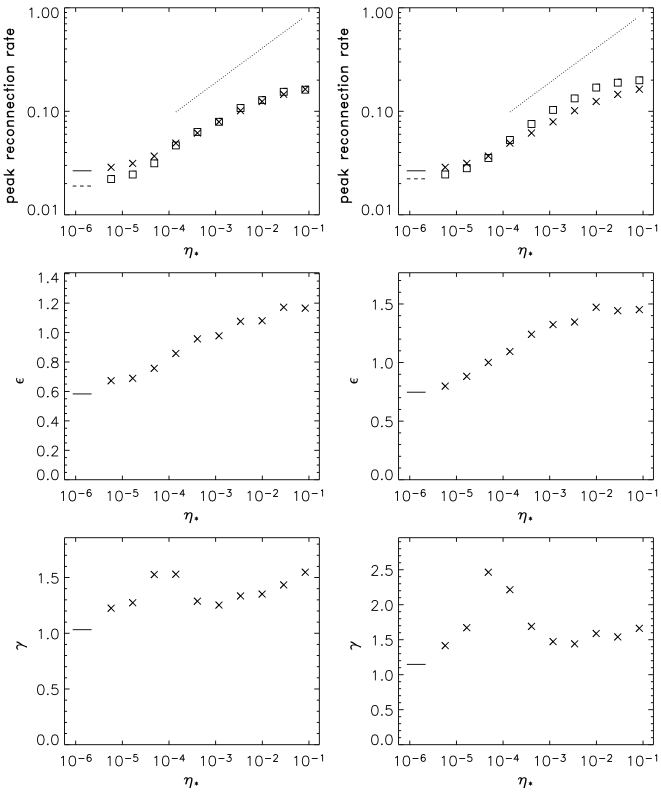

FIG. 3: Three left plots: the reconnection rate (left-top), coefficient ϵ (left-central) and coefficient γ (left-bottom) as functions of $\eta_\star$ at fixed $\eta_s = 0.0002$ and $j_c = 17.100$. The crosses and boxes show the results of our simulations and theory respectively. The solid/dashed horizontal lines correspond to $\eta_\star = 0$ and simulations/theory. The inclined dotted line given in the reconnection rate plot shows the $\propto \eta_\star^{1/3}$ scaling. Point M (see Fig. 1) is chosen to satisfy $(\eta j_z)_m = (1/3)\eta_o j_o$. Three right plots: the same as the three left plots except point M is chosen to satisfy $(\eta j_z)_m = (1/10)\eta_o j_o$.

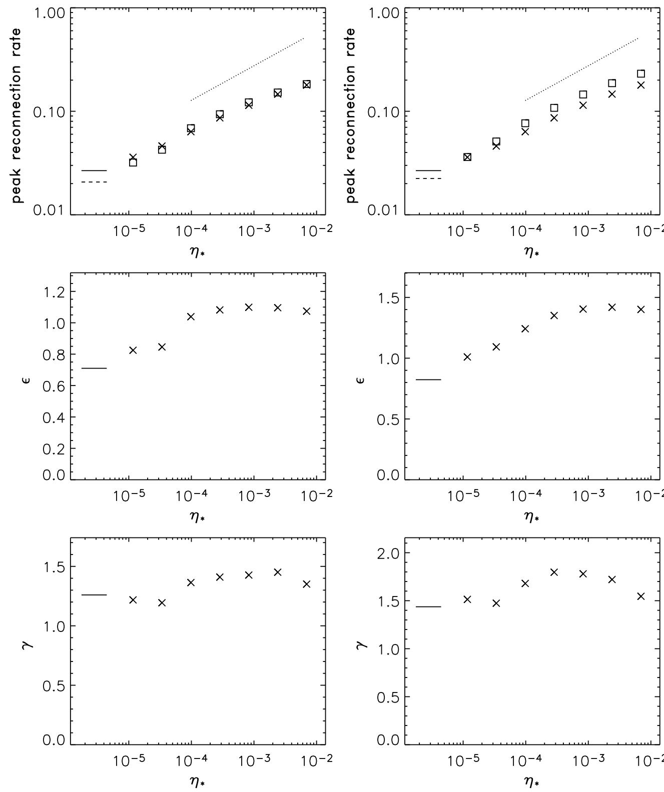

FIG. 4: These plots are the same as those in Fig. 3, except here $j_c = 4.135$.

where, as explained above, in our numerical simulations we choose $B_0 = 1$, $R_0 = 1$, $V_{A0} = 1$ and $\rho_0 = 1$, and by definition the global field scale is $L \equiv \sqrt{-2B_m/(\partial^2 B_y/\partial y^2)_m}$. We also assume that $j_o > j_c$, which is the case that we consider in our numerical simulations. As we can see from equation (34), the theoretical reconnection rate $\eta_o j_o$ is rather sensitive to B_m and L, which are the strength and scale of the magnetic field at point M outside the reconnection layer (see Fig. 1). Therefore, in order to compare the theoretical results with the results of our simulations, we need to accurately calculate the B_m and L observed in the simulations. As a result, the choice of the exact position of point M, at which B_m and L are calculated, is important. First, in our simulations we choose the point M to be the point on the x-axis at which the observed resistivity term ηj_z is three times smaller than that observed at the central point O, i.e. $(\eta j_z)_m = (1/3)\eta_o j_o$. The three plots on the left in Fig. 3 demonstrate our results for this choice. The top plot on the left shows the reconnection rate. The crosses are a log-log plot of the maximal (peak) reconnection rate observed in our simulations as a function of parameter $\eta_\star$ for fixed $\eta_s = 0.0002$ and $j_c = 17.100$. The boxes are the theoretical reconnection rate, which is given by equation (34) with the appropriate values of B_m, L and density ρ observed in the simulations. The solid horizontal line (simulations) and the dashed horizontal line (theory) correspond to the $\eta_\star = 0$ case. The inclined dotted line demonstrates the $\propto \eta_\star^{1/3}$ scaling [refer to Eq. (29)]. The crosses and the boxes do not follow the $\propto \eta_\star^{1/3}$ scaling for large values of $\eta_\star$ simply because in this case the reconnection rate becomes relatively fast and the magnetic field B_m outside of the reconnection layer is not piled up as much as in the case when $\eta_\star$ is small and the reconnection rate is relatively slow. As a result, our rate curves flatten at large values of $\eta_\star$. The central and the bottom plots on the left in Fig. 3 show the observed values of coefficients ϵ and γ, which are directly calculated from the simulation data by using equations (10) and (17). As we can see, ϵ and γ are of order of unity, as one expects. The three plots on the right in Fig. 3 are the same as the three plots on the left except point M is now chosen as the point on the x-axis at which $(\eta j_z)_m = (1/10)\eta_o j_o$. Comparing the plots on the left and the plots on the right, we see that the choice of point M is indeed important. Note that for the choice $(\eta j_z)_m = (1/3)\eta_o j_o$ for the position of point

M the half-thickness of the reconnection layer δ_o, defined as the abscissa of point M, increases from 0.011 to 0.050 as $\eta_\star$ increases from zero to its maximal value shown on the plots in Fig. 3. At the same time, for the choice $(\eta j_z)_m = (1/10)\eta_o j_o$ for the position of point M δ_o ranges from 0.018 to 0.056, which is noticeably larger. Perhaps simulations of forced reconnection with a strict control of position of point M together with control of the outside field B_m and its scale L, could be better suited for comparison to our theoretical model. Such simulations are beyond the scope of this paper. However, see more discussion of forced reconnection in the next section. Finally, Figure 4 shows the same results as Fig. 3, except the former has plots for a smaller value of the critical current, $j_c = 4.135$.

We believe that the results presented in Figs. 3 and 4 generally confirm our theoretical model. In particular, in all cases the theoretical reconnection rates and the rates observed in the simulations do not differ by more than 33%. The observed relatively small discrepancy between the theoretical and simulated rates is mainly due to the coefficient ϵ not being precisely constant in the simulations, while the variations of coefficient γ are somewhat less important [see Eq. (23) for the theoretical reconnection rate]. This discrepancy can be due to two causes. First, our theoretical model is general, but approximate, and second, the plasma is compressible in the simulations, while it is assumed to be incompressible in the theoretical model.

VI. DISCUSSION AND CONCLUSIONS

Let us summarize our main results. In this paper we take a new theoretical approach to the calculation of the rate of quasi-stationary magnetic reconnection. Our approach is based on analytical derivations of the reconnection rate from the resistive MHD equations in a small region of space that is localized about the center of a thin reconnection layer and has its size equal to the layer thickness. Our local-equations approach turns out to be feasible and insightful. It allows us to consider magnetic reconnection with an arbitrary anomalous resistivity and to calculate the reconnection rate for this general case [see Eq. (18)]. We find the interesting and important result that if plasma is incompressible and reconnection is quasi-stationary, then the reconnection rate is determined by the anomalous resistivity function $\eta(j,x,y)$ and by the strength and structure of the magnetic field just outside of the reconnection layer (i.e. at point M in Fig. 1). Thus, we find that the global magnetic field and its configuration are not directly relevant for the purpose of calculation of a quasi-stationary reconnection rate, although, of course, the local magnetic field outside the reconnection layer depends on the global field.

One of the major results of this paper is that in the case of constant resistivity, $\eta \equiv \text{const} = \eta_o$, the magnetic reconnection rate is the slow Sweet-Parker reconnection rate and not the fast Petschek reconnection rate [refer to Eqs. (28)]. This result agrees with numerical simulations and at the same time contradicts the result of the original Petschek theoretical model. In the framework of our theoretical approach, based on local equations, the reason for this contradiction can be understood as follows: In the Petschek model our parameter $\upsilon \equiv (\partial V_y/\partial y)_o = -(\partial V_x/\partial x)_o$, which is equal to the first order partial derivatives of the incompressible plasma velocities at the reconnection layer center, is basically treated as a free parameter. This is because in the Petschek model υ can be estimated as the ratio of the plasma outflow velocity (equal to the Alfven velocity for viscosity-free plasma) and the reconnection layer length, $\upsilon = (\partial V_y/\partial y)_o \approx V_A/L'$, and the layer length L' is treated as a free parameter by Petschek. In his model L' is taken to be equal to the minimal possible value, that the Petschek shocks do not seriously perturb the magnetic field in the upstream region. This is $L' \approx (L/S_o)(\ln S_o)^2$, where $S_o = V_A L/\eta_o$ is the Lundquist number [3, 5]. In this case $\upsilon \approx (V_A^2/\eta_o)(\ln S_o)^{-2}$ and, according to equations (19) and (20), the reconnection velocity in this case is equal to $V_R \approx V_A(\ln S_o)^{-1}$, which is the Petschek result. On the other hand, in our theoretical model the parameter υ is not treated as a free parameter. In fact, our three physical parameters $\upsilon \equiv (\partial V_y/\partial y)_o$, $\beta \equiv (\partial B_x/\partial y)_o$ and $j_o \equiv j_z(x=0, y=0)$ are connected to each other and must be calculated from equations (10), (15) and (16). Let us discuss the meaning of these equations. Equation (10) is the equation of magnetic energy conservation. It says that the rate of supply of the magnetic field energy into the reconnection layer υB_m^2 must be equal to the rate of the resistive dissipation of this energy $\eta_o j_o^2$. In the Petschek model υ and, accordingly, the rate of the magnetic energy supply υB_m^2 are basically prescribed by hand (resulting in an *ad hoc* fast reconnection), while in our model they are self-consistently calculated from the MHD equations. Equation (15) is the equation of plasma acceleration along the reconnection layer. It says that the magnetic tension force βj_o must be large enough in order to be able to push out all the plasma along the layer that is supplied into the layer. Finally, equation (16) is the equation of spatial homogeneity of the electric field z-component along the reconnection layer. This equation sets an upper limit on the product $\upsilon\beta$ in the case of a quasi-stationary reconnection and is directly related to the calculations and arguments given by Kulsrud [5] in the framework of the global-equations theoretical approach, see Ref. [43]. As a result, none of parameters υ, β and j_o can be treated as free parameters, and all of them must be self-consistently determined from the MHD equations.

It is very instructive to briefly examine our results from the two distinct points of view in connection with the reconnection problem, which are expressed in numerous papers on computer simulation of magnetic reconnection. These two points of view are: unforced (free) magnetic reconnection and forced magnetic reconnection. In the

case of unforced reconnection, one should solve our main equation (18) for the current j_o at the reconnection layer center and then solve for the reconnection velocity V_R by using equation (19). The solution for j_o and V_R will depend on B_m, which is the strength of the magnetic field outside the reconnection layer and which enters the right-hand-side of equation (18). On the other hand, in the case of forced magnetic reconnection the reconnection velocity V_R is prescribed and fixed. In this case the magnetic field outside the reconnection layer B_m should be treated as an unknown quantity, and equations (18) and (19) should be solved together in order to find the correct quasi-stationary values of j_o and B_m. In other words, in the forced reconnection case an initially weak outside magnetic field B_m gets piled up to higher and higher values until the resulting current j_o in the reconnection layer becomes large enough to be able to exactly match the prescribed reconnection velocity V_R and to be able to reconnect all magnetic flux and magnetic energy, which are supplied into the reconnection region in the quasi-stationary reconnection regime.

Finally, a couple of words about plasma viscosity and guide field and their effect on magnetic reconnection. First, according to our equations (18) and (19), in the case when the resistivity is constant, $\eta \equiv \text{const} = \eta_o$, and the plasma viscosity is much larger than resistivity, $\nu \gg \eta_o$, the reconnection velocity becomes $V_R/V_A \approx S_o^{-1/2}(\eta_o/\nu)^{1/4}$, which is $\sqrt[4]{\nu/\eta_o}$ times smaller than the Sweet-Parker reconnection velocity given by formula (28), see [26]. Thus, we see that the reconnection rate becomes smaller when the plasma viscosity becomes large. However, note that in many astrophysical and laboratory applications plasmas are very hot and highly rarefied. Under these conditions the ion gyro-radius becomes much shorter than the ion mean-free-path, and the plasma becomes strongly magnetized. As a result, the plasma viscosity becomes the Braginskii viscosity, which is dominated by magnetized ions [32]. In this case in all our equations above the isotropic viscosity ν, which is proportional to the ion mean-free-path, should be replaced by the Braginskii perpendicular viscosity, which is proportional to the ion gyro-radius and is much smaller than the perpendicular viscosity in a strongly magnetized plasma. Second, according to our results, in two-and-a-half dimensional geometry the guide field B_z has no effect on the quasi-stationary reconnection rate. Indeed, in our derivations the guide field appears only as magnetic pressure $B_z^2/2$ term in addition to the plasma pressure. The combined pressure P enters equations (11) and (12) of plasma acceleration along the reconnection layer and the value of spatial derivative of P is given by equation (13), which does not involve B_z. Thus, the guide field gets eliminated and does not enter into our final equation (18) for the reconnection rate. However, if one assumes that the anomalous resistivity η depends on x- and y-components of the current $j_x = \partial B_z/\partial y$ and $j_y = -\partial B_z/\partial x$ in addition to its dependence on the z-component of the current j_z, then the reconnection rate will depend on the guide field B_z.

In this paper we consider quasi-stationary magnetic reconnection in a thin reconnection layer. We leave a study of tearing modes instability in a reconnection layer and non-quasi-stationary reconnection for a future paper.

Acknowledgments

It is our special pleasure to thank Ellen Zweibel and Dmitri Uzdensky for many stimulating discussions and useful comments. We are grateful to Zoran Mikic and Samuel Vainshtein for suggesting to us the convenient computational setup used in our simulations. We would also like to thank Andrey Beresnyak, Amitava Bhattacharjee, Stas Boldyrev, Fausto Cattaneo, Jeremy Goodman, Hantao Ji, Alexander Obabko, Robert Rosner and Masaaki Yamada for a number of valuable comments. This work was supported by the Center for Magnetic Self-Organization (CMSO) grant. The numerical simulations were supported by a Center for Magnetic Reconnection Studies (CMRS) grant. The software used in this work was in part developed by the DOE supported ASC/Alliances Center for Astrophysical Thermonuclear Flashes at the University of Chicago. The simulations were carried out on DOE computers at the Oak Ridge National Laboratory.

APPENDIX A: DERIVATION OF EQUATIONS (13) AND (14)

Below, for brevity, we assume that spatial derivatives are to be taken with respect to all indexes that are listed after the comma signs in the subscripts, e.g. $V_{x,yy} \equiv \partial^2 V_x/\partial y^2$.

We derive equation (13) first. The derivation is somewhat analogous to the Sweet-Parker derivation of the pressure decrease along the reconnection layer, which leads to equation (4). Namely, to find the pressure decrease and the pressure second derivative along the layer, we integrate the pressure gradient vector along the contour O→M→M̃→Õ shown in Fig. 1 and use the force balance condition for the plasma across the reconnection layer. Now we carry out these calculations in a mathematically precise way.

For infinitesimally small values of the y-coordinate, taking into account the symmetry of the reconnection layer with respect to the x- and y-axes and plasma incompressibility, we use the following Taylor expansions in y for the plasma velocity $\mathbf{V}(x,y)$ and for the magnetic field $\mathbf{B}(x,y)$:

$$
\begin{aligned}
V_x &= V_x^{(0)}(x) + (y^2/2)V_{x,yy}^{(0)}(x) + (y^4/24)V_{x,yyyy}^{(0)}(x),\\
B_x &= yB_{x,y}^{(0)}(x) + (y^3/6)B_{x,yyy}^{(0)}(x),\\
V_y &= -yV_{x,x}^{(0)}(x) + (y^3/6)V_{y,yyy}^{(0)}(x),\\
B_y &= B_y^{(0)}(x) + (y^2/2)B_{y,yy}^{(0)}(x),
\end{aligned}
\tag{A1}
$$

where the variables with the superscripts ${}^{(0)}$ are taken at $y=0$ and depend only on x. Assuming quasi-stationarity of reconnection ($\partial/\partial t=0$) and plasma incompressibility, the MHD equation for the plasma velocity $\mathbf{V}$ is

$$\begin{aligned}\nabla P+\nabla(B_x^2+B_y^2)/2 &= -\rho(\mathbf{V}\nabla)\mathbf{V}+(\mathbf{B}\nabla)\mathbf{B} \\ &\quad +\rho\nu\nabla^2\mathbf{V}, \qquad \text{(A2)}\end{aligned}$$

where P is the sum of the plasma pressure and the z-component field magnetic pressure $B_z^2/2$. Let us calculate line integrals of the left- and right-hand-sides of equation (A2) along the contour O→M→M̃→Õ shown in Fig. 1. First, the line integral of the left-hand-side is obviously

$$\begin{aligned}&P(0,\tilde{y})-P(0,0)+(1/2)B_x^2(0,\tilde{y}) \\ &\qquad =(\tilde{y}^2/2)[P_{,yy}(0,0)+\beta^2], \qquad \text{(A3)}\end{aligned}$$

where $\tilde{y}$ is the y-coordinate of points M̃ and Õ, and we use the formulas $B_y\equiv 0$ on the y-axis, $B_x=0$ at point O and $B_x(0,y)=\beta y$ for small y [see the definition of β in Eq. (15)]. Second, using expansion formulas (A1), we calculate the following line integrals along the contour O→M→M̃→Õ, up to the second order in $\tilde{y}$:

$$\begin{aligned}\int[\rho(\mathbf{V}\nabla)\mathbf{V}]\mathbf{dl} &= \rho\frac{\tilde{y}^2}{2}\Big(\big[V_{x,x}^{(m)}\big]^2-V_x^{(m)}\big[V_{x,xx}^{(m)}+V_{x,yy}^{(m)}\big] \\ &\quad +2\int_O^M V_{x,x}^{(0)}V_{x,yy}^{(0)}\,dx\Big), \qquad \text{(A4)}\end{aligned}$$

$$\begin{aligned}\int[(\mathbf{B}\nabla)\mathbf{B}]\mathbf{dl} &= \frac{\tilde{y}^2}{2}\Big(B_y^{(m)}B_{y,yy}^{(m)}+\beta^2+B_{x,y}^{(m)}j_z^{(m)} \\ &\quad -\int_O^M\big[B_y^{(0)}B_{x,yyy}^{(0)} \\ &\qquad +B_{x,y}^{(0)}B_{y,yy}^{(0)}\big]dx\Big), \qquad \text{(A5)}\end{aligned}$$

$$\begin{aligned}\int[\rho\nu\nabla^2\mathbf{V}]\mathbf{dl} &= \rho\nu\frac{\tilde{y}^2}{2}\Big(2V_{y,yyy}^{(m)}-V_{x,xxx}^{(m)}-V_{y,yyy}^{(0)}(0) \\ &\quad -\int_O^M V_{x,yyyy}^{(0)}\,dx\Big), \qquad \text{(A6)}\end{aligned}$$

where the variables with the superscripts ${}^{(m)}$ are calculated at point M (see Fig. 1).

Next we estimate the terms on the right-hand-sides of Eqs. (A4)-(A6). Recall the notations L' and δ_o for the half-length and half-thickness of the reconnection layer (see Fig. 1), and that $\delta_o/L'\ll 1$ (which is our assumption of a thin reconnection layer). The z-current inside the reconnection layer is approximately equal to $j_o\approx B_m/\delta_o$ [see Eq. (3)], where $B_m=B_y^{(m)}$ is the field at point M, while the z-current outside the layer is $j_z^{(m)}\lesssim B_m/L'$. The last two terms on the right-hand-side of equation (A5) can be estimated as $B_{x,y}^{(m)}j_z^{(m)}\sim\beta B_m/L'\sim\beta j_o(\delta_o/L')\ll\beta j_o$ and $\int_O^M[B_y^{(0)}B_{x,yyy}^{(0)}+B_{x,y}^{(0)}B_{y,yy}^{(0)}]dx\sim\delta_o B_m\beta/L'^2\sim\beta j_o(\delta_o/L')^2\ll\beta j_o$. Next, from equation (1) with the resistivity term dropped we see that outside the reconnection layer the typical scale of the plasma velocity $\mathbf{V}$ is about the same as the typical scale of the magnetic field $\mathbf{B}$ and, therefore, can not be smaller than L'. Thus, the estimates of the three terms on the right-hand-side of equation (A4) are $[V_{x,x}^{(m)}]^2\sim V_x^{(m)}[V_{x,xx}^{(m)}+V_{x,yy}^{(m)}]\sim V_R^2/L'^2\sim\upsilon^2(\delta_o/L')^2\ll\upsilon^2$ [see Eq. (8)] and $\int_O^M V_{x,x}^{(0)}V_{x,yy}^{(0)}\,dx\sim\delta_o\upsilon V_R/L'^2\sim\upsilon^2(\delta_o/L')^2\ll\upsilon^2$. The estimates of the four terms on the right-hand-side of equation (A6) are $V_{y,yyy}^{(m)}\sim V_{x,xxx}^{(m)}\sim V_R/L'^3\sim\upsilon\delta_o/L'^3\ll\upsilon/\delta_o^2$, $V_{y,yyy}^{(0)}(0)\sim\upsilon/L'^2\ll\upsilon/\delta_o^2$ and $\int_O^M V_{x,yyyy}^{(0)}\,dx\sim\delta_o V_R/L'^4\sim\upsilon\delta_o^2/L'^4\ll\upsilon/\delta_o^2$. Note that here we use L' for estimation of y-derivatives. In fact, using the global scale L of the magnetic field outside the reconnection layer would have been more appropriate for some of the estimations (as shown in Appendix B). However, using $1/L'\geq 1/L$ for the upper estimates of the $\partial/\partial y$ derivatives is perfectly fine for the purposes in this appendix.

Next, calculating the line integral of the right-hand-side of Eq. (A2) by using formulas (A4)-(A6) and our estimates made in the previous paragraph, and then equating the result to the right-hand-side of Eq. (A3), we easily obtain equation (13). Note that the first term on the right-hand side of equation (13) can also be written in terms of the second derivative of the magnetic pressure at point M: $B_m(\partial^2B_y/\partial y^2)_m=(\partial^2/\partial y^2)(B_y^2/2+B_x^2/2)_m-\beta^2=(\partial^2/\partial y^2)(B_y^2/2+B_x^2/2)_m+\mathrm{o}\{\beta j_o\}$ (note that $\beta\ll j_o$ because the reconnection layer is thin). Therefore, as noted by Zweibel [33], equation (15) is similar to Bernoulli's equation.

Now we derive equation (14), which gives an approximate estimate of the viscosity term $\rho\nu\left[\nabla^2(\partial V_y/\partial y)\right]_o$ in equation (12). We make this estimate as follows: Note that $V_{y,yx}=0$ on the y-axis because of the symmetry of the problem relative to this axis. Therefore, from the second order Taylor expansion of $V_{y,y}(x,0)$ in x, we obtain an approximate formula $V_{y,yxx}(0,0)\approx[V_{y,y}(\delta_o,0)-V_{y,y}(0,0)]/\delta_o^2\approx -V_{y,y}(0,0)/\delta_o^2=-\upsilon/\delta_o^2$, where we take into account that $V_{y,y}(\delta_o,0)\sim V_R/L'\approx\upsilon\delta_o/L'\ll\upsilon$. We can rewrite this approximate formula for $V_{y,yxx}(0,0)$ as the following exact formula: $V_{y,yxx}(0,0)=-C\upsilon/\delta_o^2$, where C is an unknown coefficient of order unity. Our numerical simulations of reconnection with constant resistivity show that C is indeed about unity if δ_o is estimated by equation (3). Thus we immediately find that $\rho\nu\left[\nabla^2(\partial V_y/\partial y)\right]_o=\rho\nu[V_{y,yxx}(0,0)+V_{y,yyy}(0,0)]\approx\rho\nu V_{y,yxx}(0,0)\approx-\rho\nu\upsilon/\delta_o^2$, which is equation (14). Here we also use $V_{y,yyy}(0,0)\sim\upsilon/L'^2\ll\upsilon/\delta_o^2$.

APPENDIX B: DERIVATION OF EQUATION (17)

Here as in Appendix A, we assume that spatial derivatives are to be taken with respect to all indexes that are listed after the comma signs in the subscripts, e.g. $B_{x,xy}\equiv\partial^2B_x/\partial x\partial y$. We derive equation (17) in

two steps.

First, we estimate $B_{x,yyy}$ at points O and M (see Fig. 1), since we will need these estimates below. Consider the formula $B_{x,x} = -B_{y,y}$, which represents the fact that the magnetic field is divergence-free. Take the $\partial/\partial y$ and $\partial^3/\partial y^3$ derivatives of this formula and integrate the resulting equations along the interval OM shown in Fig. 1. We obtain

$$\begin{aligned} B^{(m)}_{x,y} - \beta &= \int_O^M B_{x,yx}\,dx = -\int_O^M B_{y,yy}\,dx \\ &\approx -\delta_o B^{(m)}_{y,yy}, \end{aligned} \tag{B1}$$

$$\begin{aligned} B^{(m)}_{x,yyy} - B^{(o)}_{x,yyy} &= \int_O^M B_{x,yyyx}\,dx = -\int_O^M B_{y,yyyy}\,dx \\ &\approx -\delta_o B^{(m)}_{y,yyyy}, \end{aligned} \tag{B2}$$

where the variables with the superscripts $^{(o)}$ and $^{(m)}$ are taken at points O and M respectively and $\beta = B^{(o)}_{x,y}$ [see Eq. (15)]. Note that δ_o is the half-thickness of the reconnection layer, equal to the abscissa of point M (see Fig. 1). In making the estimates of the integrals on the right-hand-sides of Eqs. (B1) and (B2), we take into account that $B^{(o)}_{y,yy} = B^{(o)}_{y,yyyy} = 0$ because $B_y \equiv 0$ on the y-axis. Now, using Eq. (B1), we estimate that $B^{(m)}_{x,y} \approx \beta - \delta_o B^{(m)}_{y,yy}$. Let L be the global scale of the magnetic field outside the reconnection layer. Then, since point M is located outside the reconnection layer, we have $B^{(m)}_{y,yyyy} \sim \pm B^{(m)}_{y,yy}/L^2$ and $B^{(m)}_{x,yyy} \sim \pm B^{(m)}_{x,y}/L^2$. Next, using these estimates, the above estimate for $B^{(m)}_{x,y}$ and Eq. (B2), we obtain the following formula:

$$B^{(o)}_{x,yyy} \sim B^{(m)}_{x,yyy} \sim \pm\beta/L^2 \pm (\delta_o/L^2) B^{(m)}_{y,yy}. \tag{B3}$$

Second, we estimate $j_{z,yy}$ at point O. Consider Ampere's law formula $j_z = B_{y,x} - B_{x,y}$. We take the $\partial^2/\partial y^2$ derivative of this equation and integrate the result along the interval OM shown in Fig. 1. We find that

$$\begin{aligned} \int_O^M j_{z,yy}\,dx &= \int_O^M B_{y,yyx}\,dx - \int_O^M B_{x,yyy}\,dx \\ &= B^{(m)}_{y,yy} - \int_O^M B_{x,yyy}\,dx. \end{aligned} \tag{B4}$$

The integral $\int_O^M B_{x,yyy}\,dx$ can be estimated by using formula (B3). The integral of $j_{z,yy}$ can be estimated as $\int_O^M j_{z,yy}\,dx \sim \delta_o j^{(o)}_{z,yy}$. As a result, we obtain

$$\delta_o j^{(o)}_{z,yy} \approx B^{(m)}_{y,yy} \pm \delta_o \frac{\beta}{L^2} \pm \delta_o \frac{\delta_o}{L^2} B^{(m)}_{y,yy} \approx B^{(m)}_{y,yy}, \tag{B5}$$

where we use $\delta_o \ll L$ and $\delta_o\beta/L^2 = (\delta_o j_o/L^2)(\beta/j_o) \approx (B_m/L^2)(\beta/j_o) \approx \pm B^{(m)}_{y,yy}(\beta/j_o) \ll |B^{(m)}_{y,yy}|$, see Eq. (3) and note that $\beta \ll j_o$ because reconnection layer is thin. Finally, substituting an estimate $\delta_o \approx B_m/j_o$ into formula (B5), we obtain equation (17) with coefficient $\gamma \approx 1$.

As suggested by Uzdensky [34], there exists a nice graphical interpretation of the fact that the y-scale of the current j_z is about the same as the scale of the outside magnetic field, i.e. $j_o/(\partial^2 j_z/\partial y^2)_o \approx B_m/(\partial^2 B_y/\partial y^2)_m$ and that equation (17) holds. There can be two different cases of the reconnection layer geometry. First, the half-length of the reconnection layer L' can be approximately equal to the global scale L of the outside field. In this case the reconnection is Sweet-Parker and $L' \approx L$ is the only available scale in the y-direction. Therefore, in this case $j_o/|\partial^2 j_z/\partial y^2|_o \approx B_m/|\partial^2 B_y/\partial y^2|_m \approx L^2 \approx L'^2$. In the second case the reconnection layer half-length is much smaller than the global scale, $L' \ll L$, and the reconnection is fast (relative to the Sweet-Parker reconnection). In this case, the z-current $j_z(0, y)$ on the y-axis drops abruptly, as the y-coordinate passes value L' and point $(0, y)$ moves from the region inside the reconnection layer to the region of the outflowing plasma that is located between the Petschek shocks (see Fig. 1). However, the z-current j_z stays large inside the shocks. In other words, j_z is a smooth function (on the global scale L) along the lines that lie inside the reconnection layer and extend into the shock separatrices. Thus, in this case, despite $L' \ll L$, the y-scale of the z-current at the reconnection layer central point O is still L. This graphical interpretation is well demonstrated by the bottom-left plot of the current for the Petschek-Kulsrud ("P-K") reconnection case in Fig. 2.

---

[1] P. A. Sweet, in *Electromagnetic Phenomena in Ionized Gases*, edited by B. Lehnert (Cambridge University Press, New York, 1958), p. 123.
[2] E. N. Parker, Astrophys. J., Suppl. Ser. **8**, 177 (1963).
[3] H. E. Petschek, in *AAS-NASA Symposium on Solar Flares* NASA SP50 (National Aeronautics and Space Administration, Washington, DC, 1964), p. 425.
[4] D. Biskamp, Phys. Fluids **29**, 1520 (1986).
[5] R. M. Kulsrud, Earth, Planets and Space **53**, 417 (2001); astro-ph/0007075.
[6] D. A. Uzdensky and R. M. Kulsrud, Phys. Plasmas **7**, 4018 (2000).
[7] M. Ugai and T. Tsuda, J. Plasma Phys. **17**, 337 (1977).
[8] T. Tsuda and M. Ugai, J. Plasma Phys. **18**, 451 (1977).
[9] T. Hayashi and T. Sato, J. Geophys. Res. **83**, 217 (1978).
[10] T. Sato and T. Hayashi, Phys. Fluids **22**, 1189 (1979).
[11] M. Scholer, J. Geophys. Res. **94**, 8805 (1989).
[12] A. Lazarian and E. T. Vishniac, Astrophys. J. **517**, 700 (1999).
[13] E. Kim and P. H. Diamond, Astrophys. J. **556**, 1052 (2001)
[14] D. Biskamp, E. Schwarz, and J. F. Drake, Phys. Rev.

Lett. **75**, 3850 (1995).
[15] A. Bhattacharjee, Z. W. Ma, and X. Wang, 2003, in *Turbulence and Magnetic Fields in Astrophysics*, edited by E. Falgarone and T. Passot (Springer, 2003), Lecture Notes in Physics **614**, p. 351.
[16] I. J. D. Craig and P. G. Watson, Phys. Plasmas **12**, 012306 (2005).
[17] J. F. Drake, M. Swisdak, C. Cattell, M. A. Shay, B. N. Rogers, and A. Zeiler, Science **299**, 873 (2003).
[18] M. Hanasz and H. Lesch, Astron. Astrophys. **404**, 389 (2003).
[19] F. Heitsch and E. G. Zweibel, Astrophys. J. **583**, 229 (2003).
[20] B. N. Rogers, R. E. Denton, and J. F. Drake, J. Geophys. Res. **108**, 1111 (2003).
[21] M. Shay, J. Drake, B. Rogers, and R. Denton, J. Geophys. Res. **106**, 3759 (2001).
[22] R. M. Kulsrud, *Plasma Physics for Astrophysics* (Princeton University Press, 2005).
[23] H. P. Furth, J. Killeen, and M. N. Rosenbluth, Phys. Fluids **6**, 459 (1963).
[24] L. D. Landau and E. M. Lifshitz, *Electrodynamics of continuous media* (New York, Pergamon, 1983).
[25] V. M. Vasyliunas, Rev. Geophys. Space Phys. **18**, 303 (1975).
[26] W. Park, D. A. Monticello, and R. B. White, Phys. Fluids **27**, 137 (1984).
[27] J. A. Breslau and S. C. Jardin, Physics of Plasmas **10**, 1291 (2003).
[28] D. Biskamp and E. Schwarz, Phys. Plasmas **8**, 4729 (2001).
[29] Z. Mikic and S. Vainshtein, unpublished (2003).
[30] A. C. Calder, *et al.* , Astrophys. J., Suppl. Ser. **143**, 201 (2002).
[31] B. Fryxell, *et al.* , Astrophys. J., Suppl. Ser. **131**, 273 (2000).
[32] S. I. Braginskii, Rev. Plas. Phys. **1**, 205 (1965).
[33] E. G. Zweibel, private communication (2005).
[34] D. A. Uzdensky, private communication (2005).
[35] E. G. Harris, Nuovo Cimento **23**, 115 (1962).
[36] Otherwise, if $|\partial B_x/\partial y|_o \approx |\partial B_y/\partial x|_o$, then obviously the length of the layer would be of the order of its thickness.
[37] Note that if we adopt the global-derivations approach, then our additional unknown parameter $\beta \equiv (\partial B_x/\partial y)_o$ can be estimated as $\beta \approx B_x(0, L)/L \approx (\delta_o/L)B_m/L \approx (V_R/V_{out})B_m/L$, the parameter $\upsilon \equiv (\partial V_y/\partial y)_o$ can be estimated as $\upsilon \approx V_{out}/L$, and our equation (9) reduces to the Sweet-Parker equation (2), as one expects.
[38] We assume η to be a function of j_z instead of the total current $j = (j_z^2 + j_x^2 + j_y^2)^{1/2}$. This is because the reconnection process proceeds due to the z-component of the electric field, see Eq. (1), and it is reasonable to assume that the electrical conductivity in the z-direction can be reduced by plasma instabilities due to large values of j_z.
[39] Note that Eqs. (3) and (8) are exact for the Harris model reconnection sheet [35], which has $B_y = B_m \tanh(x/\delta_o)$, $B_x = 0$, $j_z = (B_m/\delta_o)\cosh^{-2}(x/\delta_o)$, $\eta = \text{const}$ and $V_x = -(\eta/\delta_o)\tanh(x/\delta_o)$.
[40] Note that the $\text{o}\{\rho\upsilon^2, \beta j_o, \rho\nu\upsilon/\delta_o^2\}$ terms can still be much larger than the $B_m(\partial^2 B_y/\partial y^2)_m$ term in equation (13), in which case the pressure term $(\partial^2 P/\partial y^2)_o$ is unimportant and negligible in equation (12). This happens when reconnection with anomalous resistivity is much faster than Sweet-Parker reconnection.
[41] The jump condition (24) was used by Kulsrud [5] for the case of a viscosity-free plasma. It can be shown from the full non-ideal MHD equations that this condition is unchanged in the case of a viscous plasma.
[42] Following Kulsrud [5], for the definition of the global magnetic field scale L we use formula $B_y(\delta_o, y) = B_m(1 - y^2/L^2)$ for the field y-component along the interval M$\tilde{\text{M}}$ that is outside the reconnection layer as shown in Fig. 1.
[43] The spatial homogeneity of the electric field z-component and the resulting upper limit on $\upsilon\beta$ are directly related to the explanation of why the Petschek reconnection model does not work, as shown by Kulsrud [5] in the framework of the global-equations. Kulsrud's argument is that the length of Petschek reconnection layer L' is not a free parameter, but must be determined by the condition that the perpendicular magnetic field component B_x has to be regenerated by the rotation of the parallel field component B_y at the same rate as it is being swept away by the downstream flow. It is easy to see that the integration of "local" equation (1) without the resistivity term over the area of the contour O→M→$\tilde{\text{M}}$→$\tilde{\text{O}}$ shown in Fig. 1 will result in the same "global" equation for the balance of the B_x field, which was used by Kulsrud in his work [5].

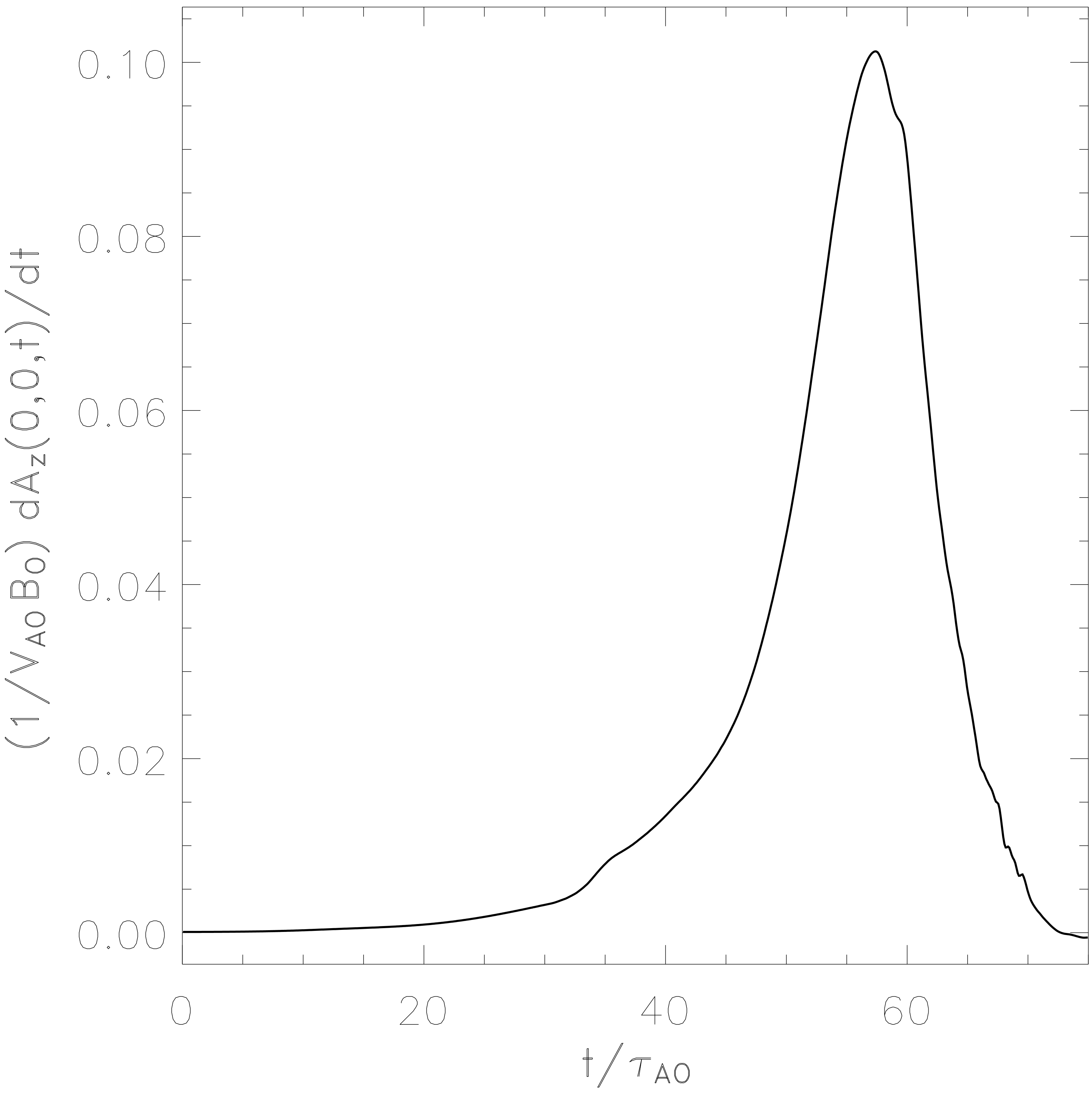
0.00
0.02
0.04
0.06
0.08
0.10
0
20
40
60
$(1/V_{A0}B_0)\ dA_z(0,0,t)/dt$
t/τ_{A0}